Supporting Information for *In-situ* electronic characterization of graphene nanoconstrictions fabricated in a transmission electron microscope.

Ye Lu[†], Christopher A. Merchant[†], Marija Drndić, A. T. Charlie Johnson

Department of Physics and Astronomy, University of Pennsylvania, Philadelphia,

Pennsylvania, 19104.

[†]These authors contributed equally to this work.

Correspondence to: Marija Drndić email: drndic@physics.upenn.edu
Correspondence to: A. T. Charlie Johnson email: cjohnson@physics.upenn.edu

1. TEM image of a sample before and after current annealing
2. TEM image of a nanopore on the graphene nanoribbon before and after current annealing
3. Control experiment to study the effects of TEM beam-induced contamination.
4. TEM images of several, few-nanometer wide, graphene nanoconstrictions (GNCs).
5. Analysis of data in Figure 4 in main text.

1. TEM image of a sample before and after current annealing

Fig S1 (a) is TEM image of surface of a graphene ribbon as fabricated. After current annealing described in the main text, the graphene surface is much cleaner, as shown in Fig S1 (b). We attribute this improvement to the removal of surface residues that vaporize when the sample undergoes Joule heating to high temperature inside the TEM vacuum chamber. The residues can occur during graphene growth and transfer to the TEM substrate, as well as during lithographic steps used to define the graphene ribbons. The cleaner surface is expected to result in reduced surface charge scattering and enhanced conductivity of the graphene and the GNCs produced by nanosculpting.
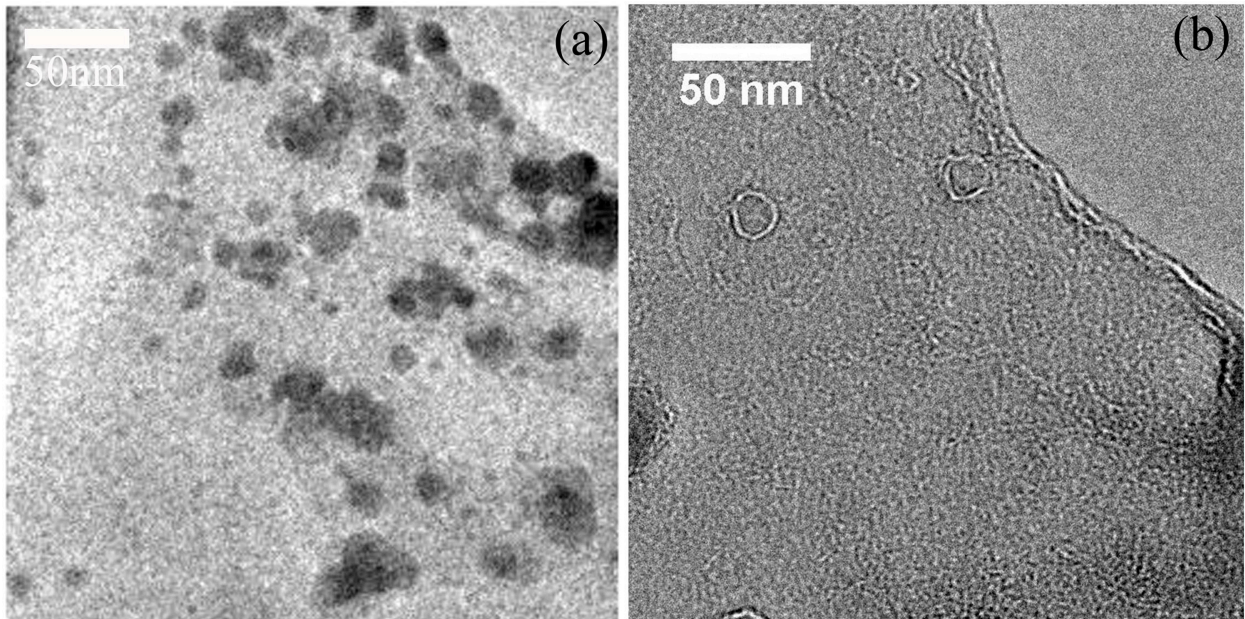

Figure S1: TEM images of a suspended graphene ribbon before (a) and after (b) current annealing.

2. TEM image of a nanopore on the graphene nanoribbon before and after current annealing.

Current annealing increases the nanoribbon temperature and induces a structural reconfiguration of the graphene. For example, Figure S2(a) is a TEM image of a round graphene nanopore before the annealing process. Fig. S2 (b) shows the faceted structure of a nominally identical pore after annealing. Nanopores recrystallize during annealing, as indicated by the hexagonal structure of the pore in Fig. S2(b) and the appearance of 60° and 120° angles along the pore edge. These FLG edge structure reconfigurations are consistent with those observed on graphitic nanoribbon experiments during material heating [1-2]. These observations suggest that during current annealing, CVD graphene may be converted to a more perfect material that resembles exfoliated graphene both structurally and electronically.
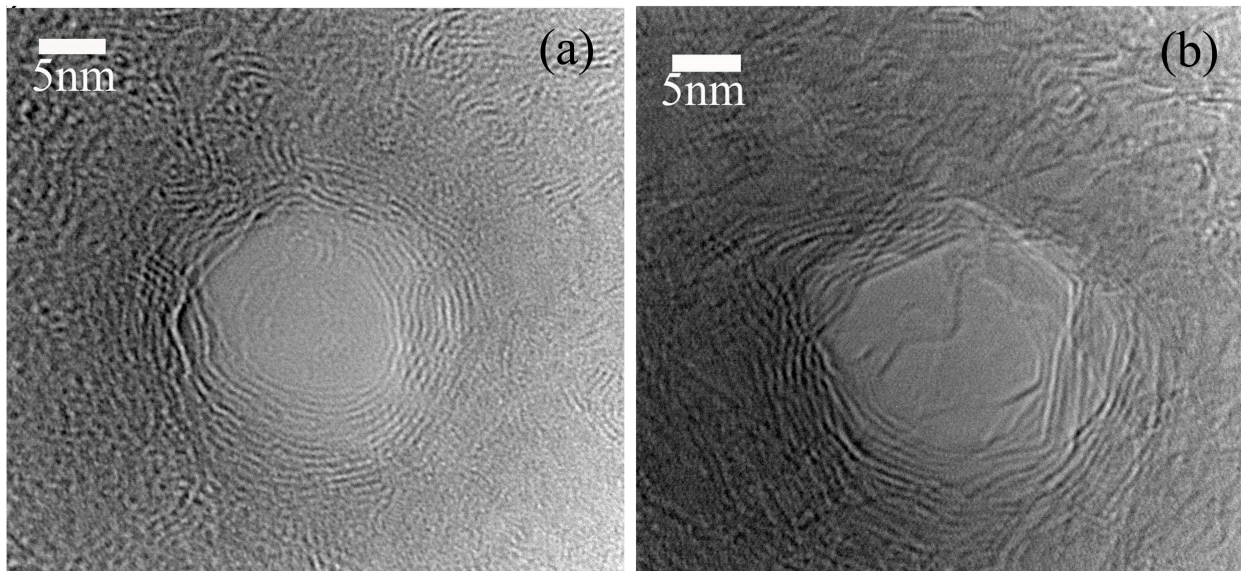

Figure S2: (a) Typical TEM images showing nanopore structural changes before and (d) after current annealing.

3. Control experiment to study the effects of TEM beam-induced contamination

A control experiment was done to rule out the possibility that the high conductance of GNC devices is due to deposition of amorphous carbon or other contamination in the TEM. Figure S3 (a) is an entirely severed graphene ribbon device. Tens of seconds of electron beam exposure was used to create a carbon bridge to reconnect the structure (Figs. S3(b) and (d)). I-V measurements of the deposited carbon bridge (Fig S3(c)) show a resistance of ~ 60 MΩ, more than three orders of magnitude higher than all the measured GNCs devices.
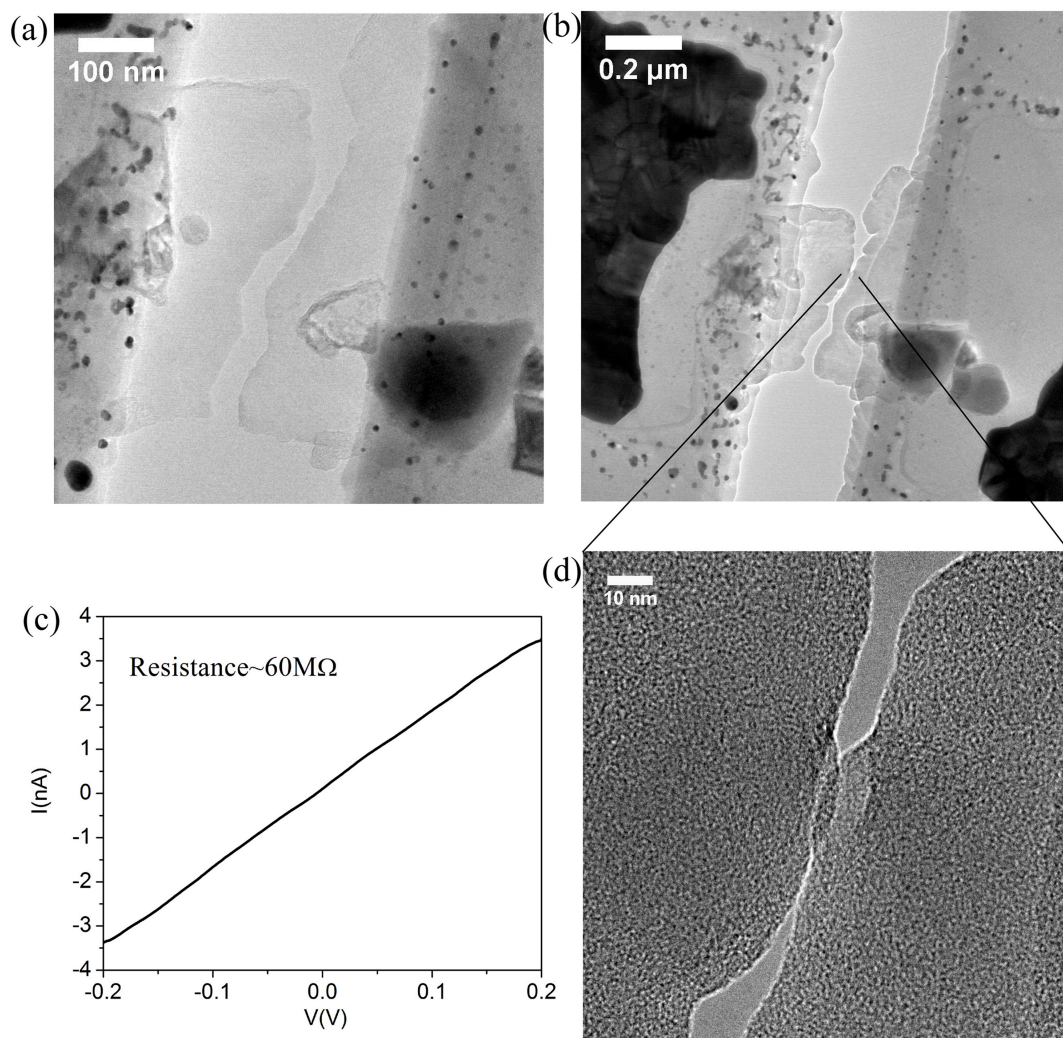

Figure S3: (a) TEM image of a severed suspended graphene ribbon. (b & d) After minutes-long electron beam exposure, the severed region is bridged by deposited carbon. (c) I-V of the contamination bridge shows it has a very high resistance compared to all GNCs measured.

4. TEM images of few-nanometer wide, graphene nanoconstrictions (GNCs)

Two graphene nanoconstrictions (GNCs) fabricated using the method described in the main text. The widths of these GNCs are ~ 6 nm and ~ 1 nm, for images in (a) and (b), respectively.
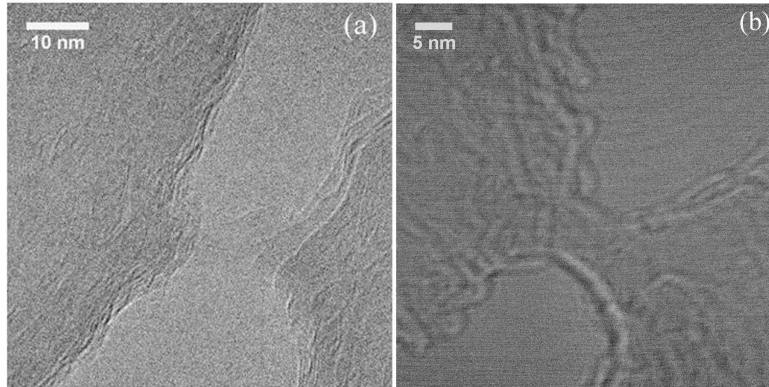

Figure S4. TEM images of two GNCs with widths of about 5 nm.

5. Analysis of resistance versus width using different power laws

We fit data presented in Fig. 4 with different power law parameters. Figure S5 (a) shows fits to the data in Figure 4(a) of the main text when α=0.25 and Figure S5 (b) is the fit when α=1. In α=0.25 case, the best fits to the data gives negative values of the contact resistance which are not physical. In α=1 case, the best fit of the data gives contact resistances which are higher than 7 measured resistances, which is also not physically possible. The power law of α=0.75 provides far superior fits, as discussed in the main text.
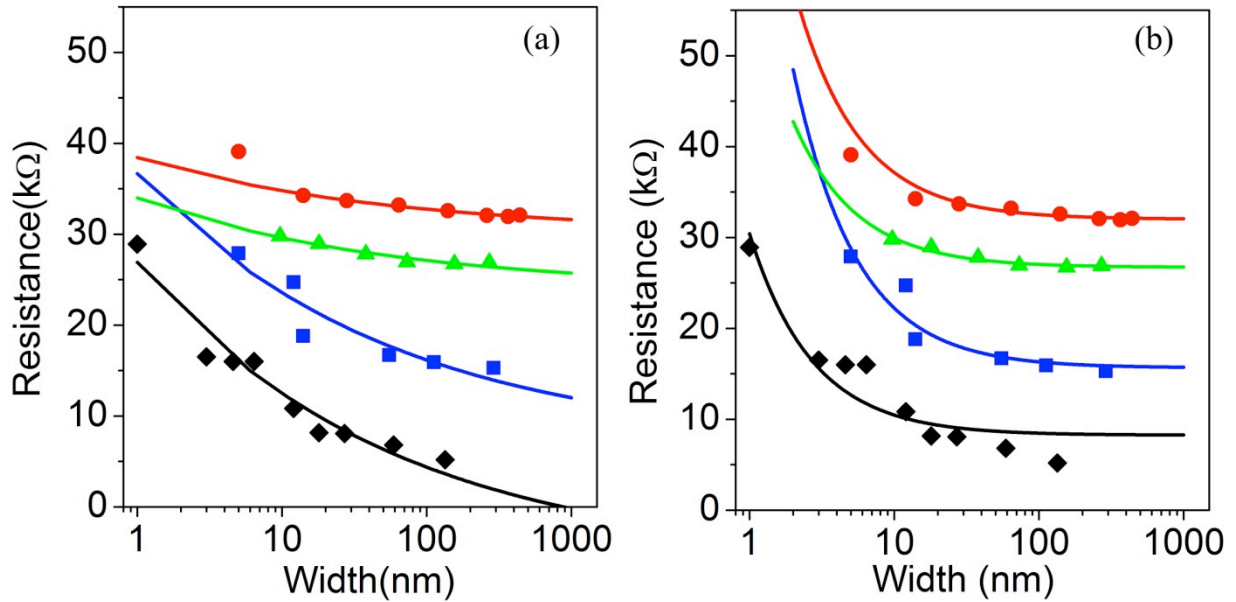

Figure S5 Fits to the data in Figure 4 in the main text where we have chosen $\alpha = 0.25$ and $\alpha = 1$. (a) Two-terminal graphene nanoconstriction resistance as a function of width. Blue, green and red data have been shifted up by intervals of 10 kΩ for clarity. Fit lines are of the form $R_{TOT} = R_C + R_M \cdot w^{-\alpha}$ with fitting parameter $\alpha = 0.25$ and w, the GNC width in nm. Best fit parameters are $R_C = -6$ kΩ (black line), $R_C = -3.4$ kΩ (blue line), $R_C = 3.9$ kΩ (blue line), $R_C = 0.13$ kΩ (red line). We can conclude that $\alpha = 0.25$ is not a good fit of our data because it frequently results in best fit contact resistances that are negative. (b) The same data fitted with fitting parameter $\alpha = 1$ and w, the GNC width in nm. $R_C = 8.25$ kΩ (black line), $R_C = 5.66$ kΩ (blue line), $R_C = 6.72$ kΩ (blue line), $R_C = 2$ kΩ (red line). The fit qualities are not satisfactory (e.g., red and black data sets), and these fits result unreasonably high contact resistances (larger than the measured resistance of the wider samples).

Figure S6(a) and S6(b) are the fits of data in Figure 4(a) and 4(b) when α=0.5, respectively. The fits are reasonable, so this power law value is not strongly ruled out, as was the case for α=0.25 and α=1. However, the fit to the data in Figure S6(b) has a R^2 value 0.82, which is not as good as the shown in Figure 4(b) in the main text (R^2=0.86).
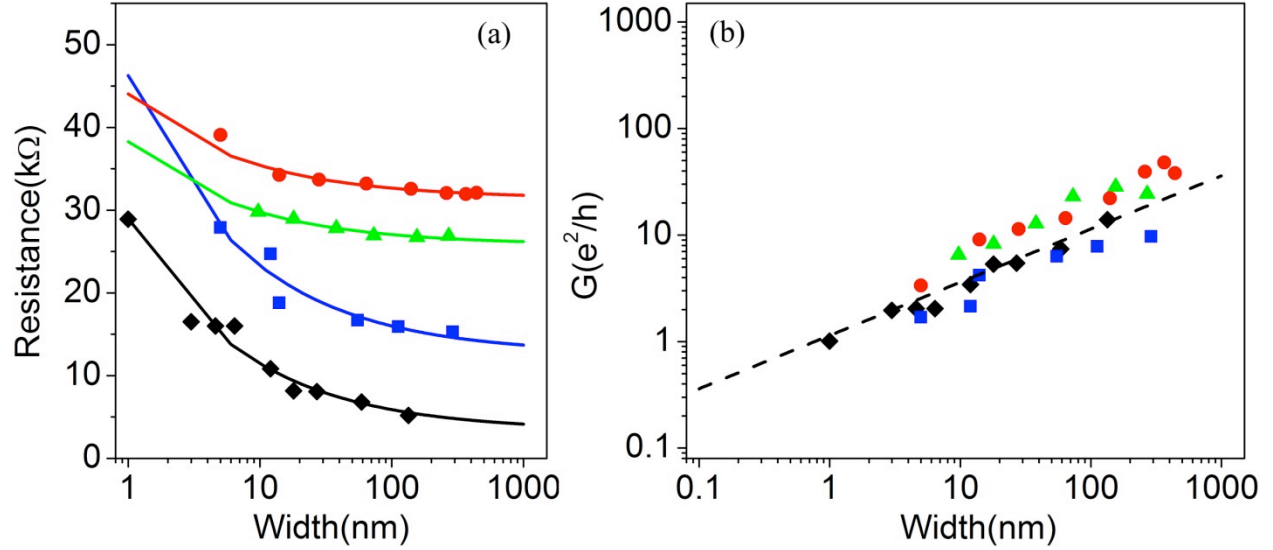

Figure S6 Data in Figure 4 in the main text fitted with parameters $\alpha = 0.5$. (a) Two-terminal graphene nanoconstriction resistance as a function of width. Blue, green and red data have been shifted up by intervals of 10 kΩ for readability and error bars are within the size of the data markers. Fit lines are of the form $R_{TOT} = R_C + R_M \cdot w^{-\alpha}$ with fitting parameter $\alpha = 0.5$ and w, the GNC width in nm. $R_C = 3.3$ kΩ, $R_M = 25$ kΩ (black line), $R_C = 2.6$ kΩ and $R_M = 34$ kΩ (blue line), $R_C = 5.8$ kΩ and $R_M = 12$ kΩ (blue line), $R_C = 1.4$ kΩ and $R_M = 13$ kΩ (red line). (b) GNC conductance as a function of width on a log-log scale. Data is taken from (a) with R_C subtracted. Dashed line is a fit of the form $G \sim 1.1\sigma_0 \cdot w^{\alpha}$ with $\alpha = 0.5$, w is the width of the GNC in nm, and $\sigma_0 = e^2/h$. Fit R^2 value is 0.82.

1.   Jia, X., et al., *Controlled Formation of Sharp Zigzag and Armchair Edges in Graphitic Nanoribbons.* Science, 2009. **323**, 1701-1705.
2.   Song, B., et al., *Atomic-Scale Electron-Beam Sculpting of Near-Defect-Free Graphene Nanostructures.* Nano Letters, 2011. **11**, 2247-2250.